*The FASEB Journal*

FASEB
Federation of American Societies for Experimental Biology

RESEARCH ARTICLE OPEN ACCESS

# NOR-1 Overexpression Elevates Myoglobin Expression via PERM1 and Enhances Mitochondrial Function and Endurance in Skeletal Muscles of Aged Mice

Hector G. Paez[1,2,3,4] | Christopher R. Pitzer[1,2,3,4] | Peter J. Ferrandi[2,4,5] | Junaith S. Mohamed[2,4,5] | Stephen E. Alway[1,2,3,4]

[1]Department of Physiology, College of Medicine, University of Tennessee Health Science Center, Memphis, Tennessee, USA | [2]Integrated Biomedical Sciences Graduate Program, College of Graduate Health Sciences, University of Tennessee Health Science Center, Memphis, Tennessee, USA | [3]Laboratory of Muscle Biology and Sarcopenia, Department of Physical Therapy, College of Health Professions, University of Tennessee Health Science Center, Memphis, Tennessee, USA | [4]Division of Rehabilitation Sciences, Center for Muscle, Metabolism and Neuropathology, College of Health Professions, University of Tennessee Health Science Center, Memphis, Tennessee, USA | [5]Laboratory of Muscle and Nerve, Department of Diagnostic and Health Sciences, College of Health Professions, University of Tennessee Health Science Center, Memphis, Tennessee, USA

**Correspondence:** Stephen E. Alway (salway@uthsc.edu)

**Received:** 8 February 2025 | **Revised:** 23 March 2025 | **Accepted:** 4 April 2025

**Funding:** This work was supported by U.S. Department of Defense (DOD) (Grant W81XWH-21-1-0187) and HHS | National Institutes of Health (NIH) (Grant R21AR079843).

**Keywords:** aging | autophagy | fatigue | mitochondria | muscle

## ABSTRACT

Skeletal muscle health and function deteriorate with age, ultimately leading to impaired mobility and disability. Exercise is among the most effective interventions to mitigate muscle dysfunction in aging and reverse deficits. However, low attrition and an impaired capacity to exercise may limit its utility in improving muscle function in aged persons. Therefore, it is crucial to advance our mechanistic understanding of the molecular transducers of exercise to identify new and innovative drug targets to improve muscle health. Transcriptomic profiling of the human response to exercise has revealed that the nuclear receptor NR4A3 (NOR-1) is among the most responsive genes to acute exercise. Previously, we observed that in vitro knockdown of NOR-1 alters metabolic signaling in C2C12 myotubes. Specifically, we found that expression of PERM1, CKMT2, myoglobin, and mTORC1 signaling were perturbed during the knockdown of NOR-1. Herein, we extend these findings and observe that a NOR-1-PERM1-myoglobin axis regulates myoglobin expression in vitro. Furthermore, we found that aging is associated with reduced skeletal muscle NOR-1 expression. Although it is well known that exercise improves aged muscle function, whether overexpression of the exercise-responsive gene NOR-1 can confer benefits and improve muscle function in an aged context has not been evaluated. We found that the overexpression of NOR-1 in aged muscle results in enhanced muscle endurance, mitochondrial respiration, and elevated expression of NOR-1 responsive genes that we previously identified in loss of function studies. However, we also observed that overexpression of NOR-1 did not improve maximal muscle torque production and resulted in a small but significant loss of muscle wet weight that was concomitant with elevated autophagy signaling. Our data suggest that NOR-1 expression may reduce muscle fatigability and that NOR-1 drives myoglobin expression in a PERM1-dependent manner.

## 1 | Introduction

Physical activity, especially exercise, is highly correlated with reduced mortality [1, 2]. In contrast, sedentary behavior, inactivity, and muscle disuse impair skeletal muscle metabolic health and can result in an enhanced risk for metabolic disease [2, 3]. Aging is associated with muscle atrophy, a loss of type 2 fiber size [4], mitochondrial dysfunction [5, 6], and impairments in muscle performance [7]. Exercise is among the most effective ways to mitigate the sequelae of muscle aging by improving muscle mass [8], mitochondrial dynamics [9], and reducing apoptotic signaling in skeletal muscle [10, 11]. Furthermore, it has been found that exercise can modulate several pathways that are implicated in aging-associated muscle dysfunction through the modulation of mTORC1 and the autophagy machinery [12–15]. For example, exercise can enhance muscle protein synthesis through mTORC1 [16] and activate autophagy as evidenced by alterations to LC3 lipidation and P62 content [15]. While exercise can combat age-associated impairments in skeletal muscle, the identification of the molecular drivers of these benefits is critical.

NOR-1 has been identified as among the most responsive genes in human skeletal muscle in response to acute aerobic and acute resistance exercise [17]. Among the top genes associated with the acute response to exercise, NOR-1 is also transcriptionally repressed in skeletal muscle during inactivity in humans [17]. Indeed, enhanced expression of NOR-1 is so drastic after exercise that it is used as a molecular marker for acute exercise validation in a number of studies [18–22]. Importantly, in vitro attempts at exercise simulation using electrically evoked stimulation [23], $Ca^{2+}$ ionophore treatment [24], and ß-adrenergic stimulation [25, 26] have all been shown to enhance NOR-1 expression in skeletal muscle cells similarly to exercise. Recently, we observed that knockdown (K.D.) of NOR-1 impairs contractile and metabolic gene expression in C2C12 myotubes [27]. To identify transcripts that are regulated by NOR-1, we compared gene sequencing data from C2C12 myotubes after NOR-1 K.D. to the gene expression data from animals that overexpress skeletal muscle NOR-1 [28]. This approach allowed us to identify differentially expressed genes that are upregulated after NOR-1 overexpression and downregulated after NOR-1 K.D [27]. Notably, our previous findings suggest that K.D. of NOR-1 leads to a marked repression of the expression of genes that are important for oxidative metabolism, including PGC-1α, TFAM, PERM1, CKMT2, and myoglobin [27]. PERM1 is known to regulate mitochondrial localization [29], function [30], and exercise adaptations [31] and was among the most upregulated genes in animals that overexpress hyperactive NOR-1 [28]. Myoglobin plays the crucial role of sustaining intramuscular oxygen to support mitochondrial oxidative phosphorylation (OXPHOS) function; however, recent findings also implicate myoglobin in the regulation of lipid metabolism [32]. Furthermore, CKMT2 plays a pivotal role in energy metabolism and mitochondrial function [33, 34]. Exercise training elevates both CKMT2 and myoglobin in a PERM1-dependent manner [31] and PERM1 expression is crucial for the exercise training-mediated enhancement of both CKMT2 and myoglobin [31]. Therefore, in this study we asked if the NOR-1-induced changes to CKMT2 and myoglobin expression require elevated PERM1 expression.

**TABLE 1** | Antibody manufacturer and item number.

| Primary antibody | Manufacture number | Secondary antibody | Manufacture number |
|---|---|---|---|
| mTOR | Cell Signaling 2972S | Anti-Rabbit IgG | Cell Signaling 7074 |
| Phospho-mTOR (Ser2448) | Cell Signaling 2971S | Anti-Rabbit IgG | Cell Signaling 7074 |
| S6 | Cell Signaling 2217S | Anti-Rabbit IgG | Cell Signaling 7074 |
| Phospho-S6 (Ser235/236) | Cell Signaling 62016S | Anti-mouse IgG | Cell Signaling 7076 |
| LC3 | Cell Signaling 4108S | Anti-Rabbit IgG | Cell Signaling 7074 |
| NR4A3/NOR-1 | Sigma-Aldrich ABE1456 | Anti-Rabbit IgG | Cell Signaling 7074 |
| Dystrophin | DSHB AB 2618170 | Anti-mouse IgG2b | Invitrogen A-21146 |
| Parkin | Cell Signaling 2132S | Anti-Rabbit IgG | Cell Signaling 7074 |
| p62 | Invitrogen MAS-46931 | Anti-Rabbit IgG | Cell Signaling 7074 |

*Note:* The antibodies used in our experiments were obtained from vendors who provided data to support their testing, and production validation. We also confirmed that the lots of the antibodies remained constant over the duration of the study. Western blots were conducted to validate that the protein band sizes were at the appropriate and predicted position.

**TABLE 2** | PCR primers.

| Gene | Primer | Sequence 5′–3′ |
|---|---|---|
| PERM1 | Forward | ATAGCTCCATGGCCCTAGCTG |
| | Reverse | TGGAAGAACCAGGGACAGAC |
| HPRT | Forward | AGGGATTTGAATCACGTTTG |
| | Reverse | TTTACTGGCAACATCAACAG |
| MYHI | Forward | TGGACCCACGGTCGAAGTTG |
| | Reverse | CCATCTCGGCGTCGGAACTC |
| MYHIIA | Forward | AAGCGAAGAGTAAGGCTGTC |
| | Reverse | CTTGCAAAGGAACTTGGGCTC |
| MYHIIB | Forward | GAAGAGCCGAGAGGTTCACAC |
| | Reverse | CAGGACAGTGACAAAGAACGTC |
| MYHIIX | Forward | GAAGAGTGATTGATCCAAGTG |
| | Reverse | TATCTCCCAAAGTTATGAGTACA |
| CKMT2 | Forward | TGTCTGAGATGACGGAGCAG |
| | Reverse | CCTGGTGTGGTCTTCCTCAT |
| Myoglobin | Forward | AGCCCACACTCTCTCCTTTTGT |
| | Reverse | CAGGGTCTCAGGGTGAGTCT |
| COQ3 | Forward | CTCTCGTGGGGTTCGTCTCC |
| | Reverse | CACCGAGTTCCCACGGCTTA |
| ATP5A1 | Forward | TTGACCTTCCTTTGCGCTCG |
| | Reverse | GCACCAACAAAGGATGACCCC |
| ANT1 | Forward | TCTGCTTCGTCTACCCGCTG |
| | Reverse | TTCCGGCCAGACTGCATCAT |
| ABRA/STARS | Forward | TCAAACGCCCCTTGCTCTC |
| | Reverse | CGTGTTCATCGGCCCACT |

*Note:* Table of genes and corresponding forward and reverse primer sequences used for qPCR analysis.

Although published data implicate NOR-1 as being a regulator of exercise-mediated adaptations, it is unknown how the expression of NOR-1 may be altered by aging, exercise duration, or contraction intensity. Furthermore, while animals that overexpress a hyperactive form of NOR-1 in skeletal muscle exhibit an endurance-trained phenotype including reduced adiposity [28] and running performance [35], it is unknown if overexpression of NOR-1 can improve muscle function in aged animals. Herein we tested whether skeletal muscle NOR-1 expression is altered in aged mice and in response to exercise duration and intensity. Furthermore, using AAV-mediated overexpression of NOR-1, we observed an enhancement of several genes associated with oxidative metabolism in C2C12 myotubes and determined that a signaling axis exists between NOR-1, PERM1, and myoglobin. Lastly, by overexpressing NOR-1 in skeletal muscle, we tested whether NOR-1 can enhance muscle function in aged mice and how overexpression of NOR-1 impacts muscle size and signaling associated with muscle aging.

**TABLE 3** | IDT predesigned quantitative PCR assays.

| Gene | Predesigned IDT primer assay ID |
|---|---|
| NR4A3 | Mm.PT.58.29947344 |
| MFN2 | Mm.PT.58.6479342 |
| PGC-la | Mm.PT.58.17390716 |
| TFAM | Mm.PT.58.17630094 |

*Note:* Table of genes and item numbers for predesigned IDT primers used for qPCR analysis.

## 2 | Methods

### 2.1 | Animals

All protocols were approved by the Institutional Animal Care and Use Committee of the University of Tennessee Health Science Center. Young (5-month-old) or aged (24-month-old) male

C57BL6 mice were obtained from Jackson Labs, MA, and used for the in vivo studies. To determine the number of animals for each experimental group to obtain statistically meaningful data, we conducted a power analysis based on our preliminary data and published data from our laboratory. The power analysis was based on variables of fiber cross-sectional area, muscle wet weight, and

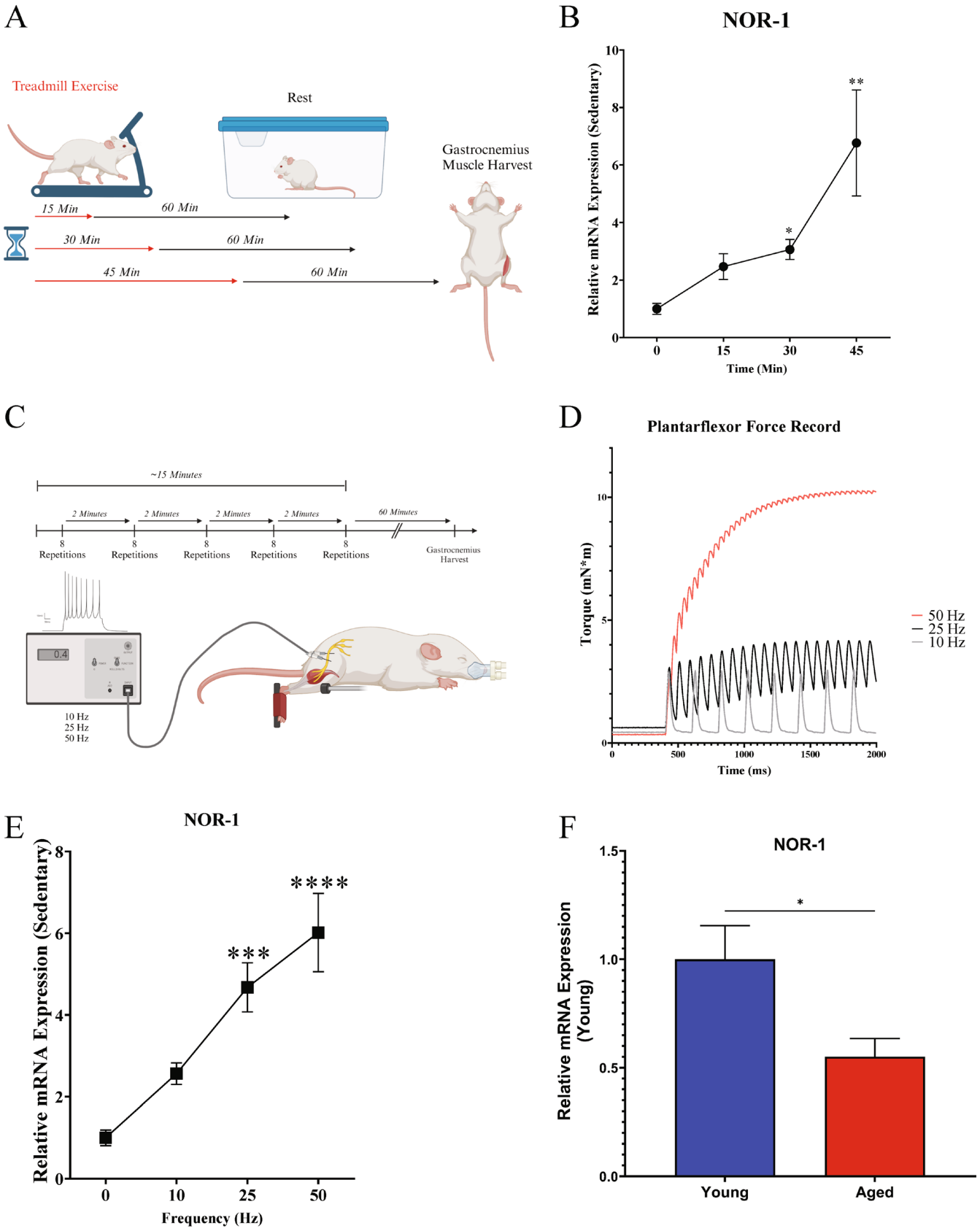


**FIGURE 1** | Legend on next page.

**FIGURE 1** | Impact of exercise duration, contraction intensity, and age on skeletal muscle NOR-1 expression. (A) Aerobic exercise design: Young (5-month-old) mice were run on a treadmill (12 m/min) for 15 ($n=4$), 30 ($n=4$), or 45 ($n=6$) minutes before undergoing a 1-h recovery prior to gastrocnemius tissue harvest. All groups of mice were compared to controls ($n=6$). (B) Expression of NOR-1 in the gastrocnemius muscle after varying times of treadmill running. (C) Isometric exercise design: Young mice were anesthetized and electrically stimulated with subcutaneous electrodes at the tibial nerve to induce isometric contraction at varying stimulation frequencies while the paw was attached to a footplate. Exercise repetition and set scheme are shown. (D) Plantar flexor force record showing a stimulation frequency-dependent increase in contraction intensity and torque production. (E) Expression of NOR-1 in the gastrocnemius muscle of mice after an electrically evoked isometric contraction of the plantar flexors at stimulation frequencies of 10 Hz ($n=3$), 25 Hz ($n=4$), and 50 Hz ($n=4$). Groups of mice were compared to non-stimulated controls ($n=6$). NOR-1 expression in the plantaris of young (9 months; $n=6$) or aged (27–31 months; $n=6$) mice. HPRT was used as a housekeeping gene. Data are presented as Mean ± SEM. Data is analyzed using Kruskall–Wallis (B) or One-Way ANOVA (E) or unpaired *t*-test (F). Statistical significance was set to $p<0.05$. *$p<0.05$, **$p<0.01$, ***$p<0.001$, ****$p<0.0001$. (A) and (C) made with Biorender.com (A) Created in BioRender. Paez, H. (2024) https://BioRender.com/q90w595 and (C) Created in BioRender. Paez, H. (2024) https://BioRender.com/u94q689.

maximal muscle force production. These a priori sample size calculations indicated that we required eight animals in each experimental group for a power of 0.80 and alpha of 0.05.

## 2.2 | Tissue Collection

At the time of euthanasia, mice were fully anesthetized (3%–5% isoflurane) and tissues were rapidly excised and weighed. The liver was harvested to verify that our local intramuscular injection of adeno-associated virus (AAV) particles did not result in off-target elevated NOR-1 protein abundance. The liver was chosen due to the strong tropism of AAV9 towards liver, and a portion of the proximal tibialis anterior muscle was stored in preservation buffer for high-resolution respirometry. The rest of the tibialis anterior muscle was frozen in 2-methylbutane cooled with liquid nitrogen. For immunoblot and qPCR analysis, the gastrocnemius muscle was cleared of excessive connective tissue, weighed, and cut into two sections before being snap frozen in liquid nitrogen and stored at −80°C. One portion of the gastrocnemius muscle was used for RNA isolation and qPCR, and another portion was used for immunoblotting.

## 2.3 | High-Resolution Respirometry

Mitochondrial oxygen flux per skeletal muscle wet weight ($pmol{\cdot}s^{-1}{\cdot}mg^{-1}$) was determined using an Oxygraph-2k High-Resolution Respirometer (Oroboros Instruments, Innsbruck, Austria) at 37°C in the oxygen concentration range of 250–550 μM in 2.0 mL of respiration medium Mir05 (0.5 mM EGTA, 3 mM $MgCl_2$, 60 mM K-lactobionate, 20 mM taurine, 10 mM $KH_2PO_4$, 20 mM HEPES, 110 mM sucrose, and 1 g/L BSA, pH adjusted to pH of 7.1 with KOH) as previously described [36]. In brief, a portion of fresh skeletal muscle tissue (1–5 mg) was cut from the proximal end of the tibialis anterior muscle and stored on ice in BIOPS preservation buffer (10 mM Ca-EGTA buffer, 0.1 μM free calcium, 20 mM imidazole, 20 mM taurine, 50 mM K-MES, 0.5 mM DTT, 6.56 mM $MgCl_2$, 5.77 mM ATP, 15 mM phosphocreatine, pH 7.1). Each muscle fiber bundle was then mechanically separated using forceps in BIOPS on ice for a maximum of 5 min. After mechanical separation, fiber bundles were permeabilized for 30 min at 4°C in saponin (50 μg/mL BIOPS) and then washed in Mir05 for 20 min. Following permeabilization, each fiber bundle was dried for 30 s on Whatman paper and weighed for a maximum of 30 s before being placed in the chamber of the high-resolution respirometer. Data were recorded using Datlab 7.3 software (Oroboros Instruments, Innsbruck, AT) at a data recording interval of 2 s. Mitochondrial respiration was assessed using the following sequential titrations of substrates, uncouplers, and inhibitors: (1) 5 mM pyruvate, 2 mM malate, and 10 mM glutamate to measure LEAK respiration supported by complex I-linked substrates ($CI_L$); (2) 5 mM ADP to determine maximal state 3 respiration supported by complex I ($CI_P$); (3) 10 μM Cytochrome C to assess the quality of the mitochondrial sample and the integrity of the mitochondrial outer membrane (data was not used from chambers if there was a > 15% increase in respiration after cytochrome C addition); (4) 10 mM succinate to determine maximal state 3 respiration with convergent electron input from complex I and II ($CI+CII_P$); (5) 0.05 μM stepwise titrations of carbonylcyanide m-cholorophenyl (CCCP) hydrazone to assess electron transfer system capacity ($CI+CII_E$); (6) 2.5 μM of Antimycin A to inhibit complex III and obtain non-mitochondrial residual oxygen consumption for normalization of all other values. Respiratory measurements were normalized to tissue wet weight immediately prior to addition into the chamber, and muscle tissue used for respirometry was taken from animals euthanized between the hours of 10:00 and 12:00 after a 5-h fast to ensure similar circadian rhythmicity across animals.

## 2.4 | Histology

Tissue cross-sections were cut at an 8 μm thickness at −20°C (CM3050S, Leica Biosystems Nussloch, Germany) and mounted on charged glass slides (ThermoFisher Scientific, Pittsburgh PA, USA) and kept at −80°C prior to immunocytochemistry as previously described [37]. Briefly, muscle sections were air dried for 10 min prior to a 10-min fixation in cold 4% paraformaldehyde (PFA) and rehydrated with PBS for 10 min before being blocked with 2.5% normal goat serum for 1 h at room temperature. Primary antibodies were obtained from the Developmental Studies Hybridoma Bank (Iowa City, IA USA) dystrophin (MANDYS8(8H11) IgG2b) and incubated overnight at 4°C. The following day, the slides were washed in PBS three times for 5 min each and then incubated in secondary Alexa Fluor antibodies (ThermoFisher Scientific Pittsburgh PA, USA) that consisted of 2 μg/mL in PBS of the Alexa Fluor anti-mouse IgG2b (A21146). The fluorescent images of the muscle cross-sections were captured with a Biotek Lionheart FX Automated Microscope (Winooski, Vermont, USA) and were imaged with emission/excitation at 628/685 nm. Cross-sectional areas and

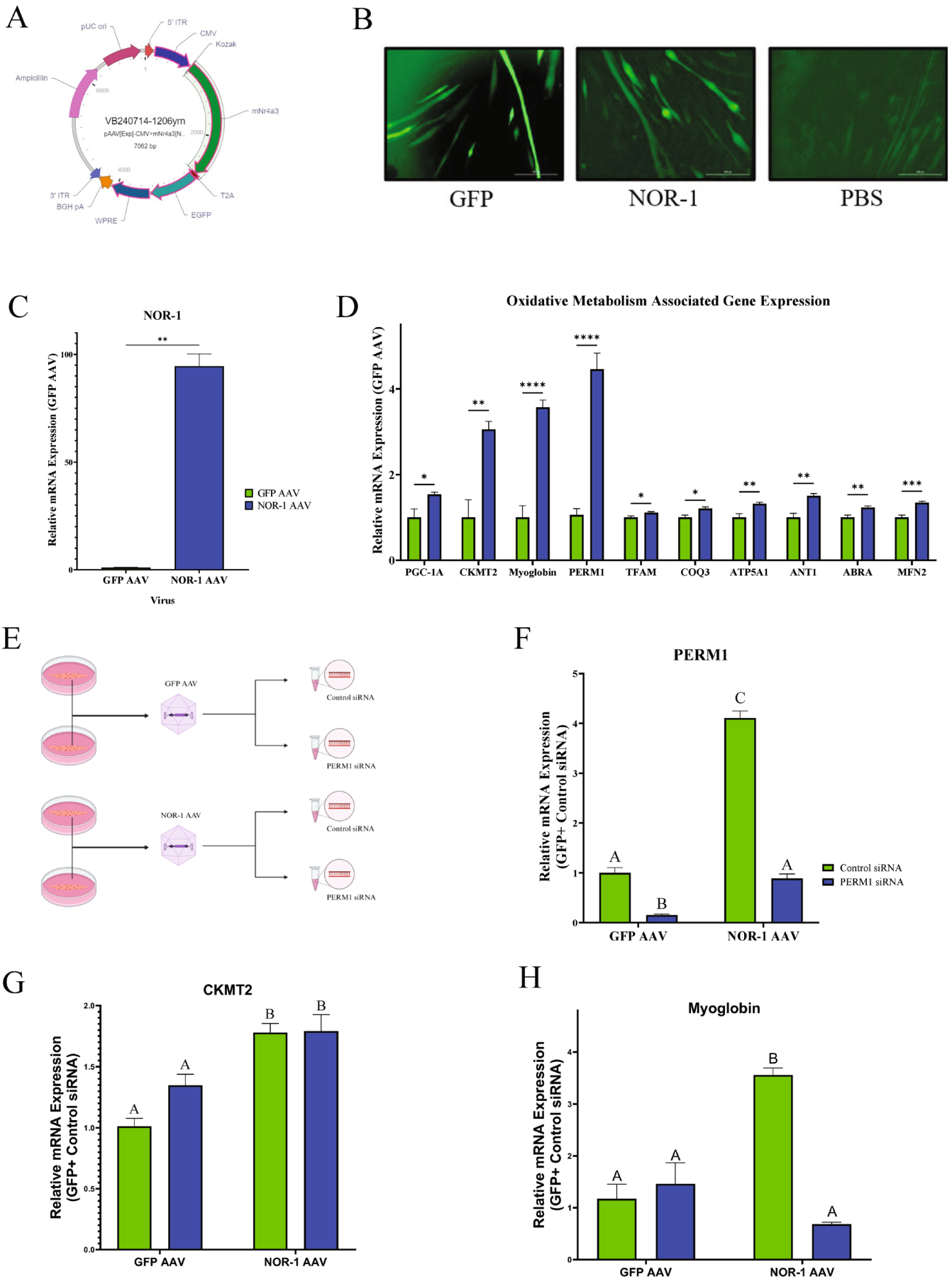


**FIGURE 2** | Legend on next page.

**FIGURE 2** | NOR-1 overexpression elevates metabolic gene expression in C2C12 myotubes. (A) Vector map of AAV9 used for NOR-1 overexpression. (B) Images showing GFP+ myotubes after AAV9 transduction. The scale bar is 200 μm. (C) NOR-1 gene expression 7 days after AAV9 transduction ($n = 6$). (D) Metabolic gene expression in C2C12 myotubes after NOR-1 overexpression ($n = 6$). (E) Experimental design: C2C12 myotubes were differentiated for 3 days before being transduced with AAVs to express either NOR-1 or GFP control protein. 5 days after transduction, NOR-1-GFP and control-GFP expressing myotubes were treated with either a PERM1 targeting or negative control siRNA for 2 days before being harvested. Expression of (F) PERM1, (G) CKMT2, and (H) myoglobin after AAV transduction and siRNA transfection ($n = 6$). HPRT was used as a housekeeping gene. Data are presented as Mean ± SEM. (C and D) are analyzed using unpaired *t*-test or unpaired *t*-test with Welch's correction when unequal variance was detected. (F–H) were analyzed using One-Way ANOVA or Brown-Forsythe and Welch ANOVA when unequal variance was detected. Statistical significance was set to $p < 0.05$. *$p < 0.05$, **$p < 0.01$, ***$p < 0.001$, ****$p < 0.0001$. Different letters (A, B, C) denote significant differences between groups. (A) The vector map was created with Vectorbuilder. (E) Made with Biorender.com (Created in BioRender. Paez, H. (2024) https://BioRender.com/g53o551).

minimum ferret diameters of GFP+ fibers in the tibialis anterior muscles were analyzed and measured using the Myovision software [38] from two to three randomly selected fields at an objective magnification of 10X.

## 2.5 | Immunoblotting

C2C12 cells and gastrocnemius muscle tissue were lysed in ice-cold RIPA buffer (ThermoScientific) containing 5 mM EDTA (ThermoFisher), and 1× Halt protease and phosphatase inhibitor cocktail (Thermo Scientific). Cell lysate protein content was measured via colorimetric quantification utilizing the DC protein assay kit (Bio-Rad). Approximately 20 μg of cell or tissue lysate was loaded and separated on SDS-polyacrylamide gels and transferred to polyvinylidene fluoride (PVDF) membranes. PVDF membranes were then stained for total protein normalization, utilizing No-Stain Protein Labeling Reagent (Invitrogen). PVDF membranes were then blocked in 5% BSA in Tris-buffered saline-Tween 20 (TBST) and total protein was fluorescently quantified via the iBright FL1500 imaging system (Invitrogen) as previously described [27]. After blocking, membranes were incubated overnight at 4°C with primary antibodies diluted at a 1:1000 concentration in Tris-buffered saline with Tween 20 (TBST). After an overnight primary antibody incubation, the membranes were incubated with anti-rabbit or anti-mouse IgG-conjugated secondary antibodies at a 1:10 000 concentration for 1 h at room temperature. Membranes were imaged and analyzed utilizing the iBright FL1500 imager and analysis software (Invitrogen). Primary and secondary antibodies are described in Table 1.

## 2.6 | RNA Isolation and Quantitative PCR

Total RNA was isolated from whole muscle or myoblasts derived from C2C12 cells using TRIzol reagent (Invitrogen) per manufacturer instructions. After phenol-chloroform extraction, RNA was precipitated using an equal volume of 70% ethanol and purified using the PureLink RNA Mini Kit (Invitrogen, Carlsbad, CA, United States) before being eluted in nuclease-free water. RNA concentration and purity (260/280 ratio) were measured using a Biotek Take3 plate (Biotek Ref. #TAKE3-SN). Any RNA sample with a 260/280 ratio below 1.9 was discarded and not utilized for PCR analysis. Approximately 1 μg of RNA was treated with DNAse to eliminate gDNA contamination and then reverse transcribed into cDNA utilizing the High-Capacity cDNA Reverse Transcription Kit (Applied Biosystems) according to manufacturer instructions. Real-time qPCR was conducted using the temperature cycle profile of 50°C for 2 min, 95°C for 10 s, followed by 40 cycles of 95°C for 15 s, and 60°C for 60 s. To validate the specificity of the amplicons, we conducted a melt curve cycle that consisted of 95°C for 15 s, 60°C for 60 s, and 95°C for 15 s. Melt curves producing multiple peaks were not included in the analysis. The relative expression levels of amplified transcripts were estimated by the comparative CT method ($2^{-\Delta\Delta CT}$). Primers that were utilized in this study can be found in Tables 2 and 3.

## 2.7 | Cell Culture Conditions

C2C12 cells were purchased from ATCC (Manassas, VA) and propagated in growth media (GM) consisting of Dulbecco's modified Eagle's medium (DMEM; Invitrogen) with 10% fetal bovine serum (FBS; Gibco) and supplemented with 1% antibiotic/antimycotic (Gibco). All cells used for experiments were > 15 passages. Cells were maintained in a humidified incubator at 37°C and 5% $CO_2$. To induce differentiation, C2C12 myoblasts were grown to 70% confluence and GM was replaced with differentiation media (DM) containing DMEM supplemented with 2% heat-inactivated horse serum (Gibco) and 1% antibiotic/antimycotic.

## 2.8 | Cell Culture Treatments

C2C12 myotubes were differentiated for 3 days prior to infection with AAV particles at an MOI of $1.6 \times 10^6$. AAV serotype 9 particles were purchased (VectorBuilder) to express the full-length NOR-1 transcript linked to an eGFP protein via a T2A linker under the control of the CMV promoter (Vector map can be found in Figure 2A). AAVs expressing eGFP under the control of the CMV promoter were used as controls. The AAVs were incubated on C2C12 myotubes for a total of 48 h prior to changing the media, and cells were harvested 7 days post-infection (10 days of differentiation). For siRNA-mediated K.D. experiments, C2C12 myotubes were treated with siRNAs starting at 5 days post-AAV infection for 48 h prior to harvest (Experimental design can be found in Figure 1E). Myotubes were transfected with 50 nM of PERM1 targeting siRNA (Qiagen, FlexiTube siRNA #S10081342) or Silencer Select Negative Control No. 1 siRNA (Invitrogen; 4390843) for 48 h utilizing lipofectamine RNAiMAX (3.5 μL/mL) (Invitrogen). We chose 7 days post-infection as our experimental time point due to the time it took to visualize GFP fluorescence in myotubes.

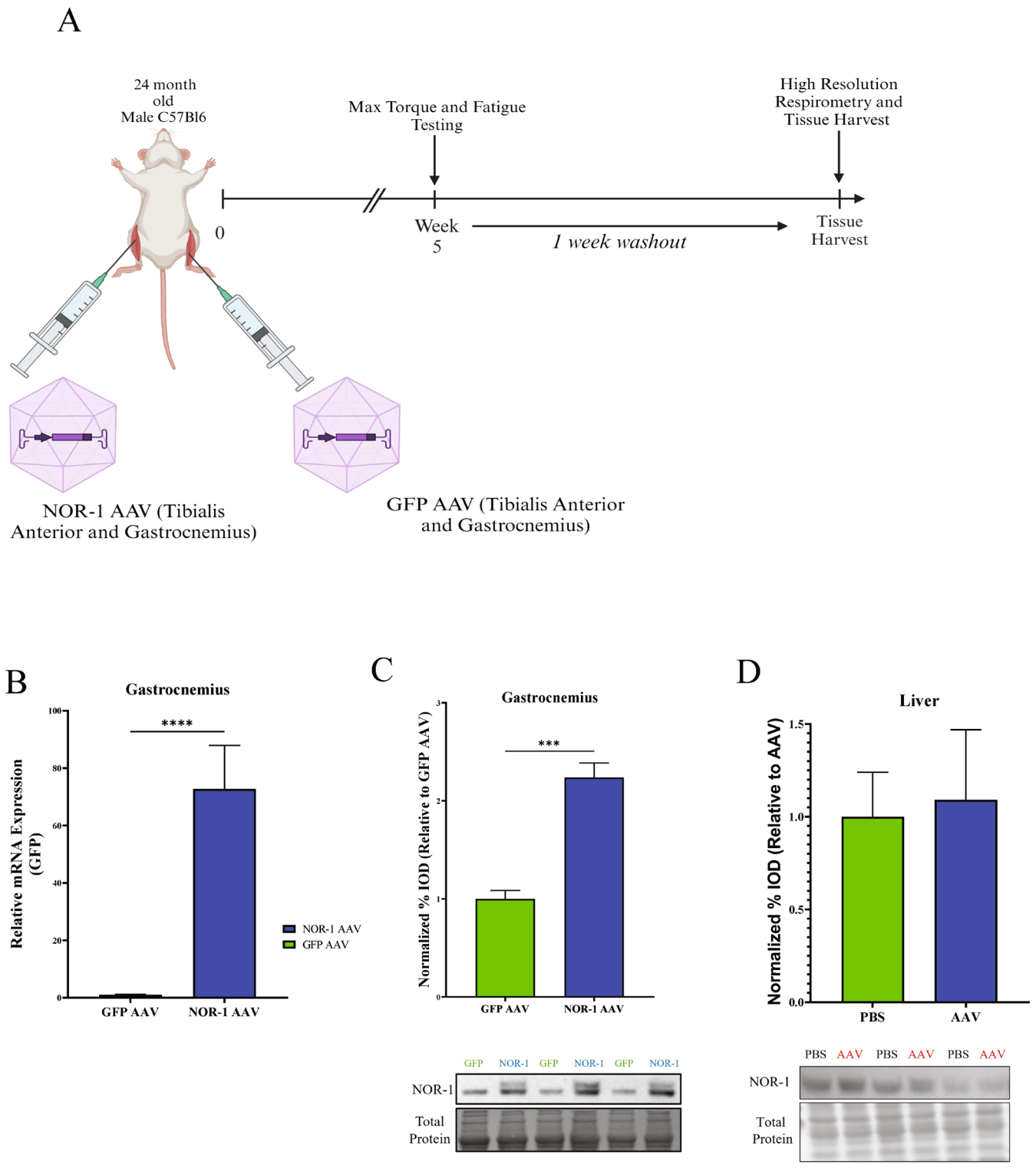


**FIGURE 3** | Overexpression of NOR-1 in vivo. (A) Experimental design: Aged (24-month-old) C57BL6 mice were injected in the tibialis anterior and gastrocnemius muscle of both hindlimbs with either an AAV to express GFP (control) or an AAV to express NOR-1 linked to a GFP protein. Functional testing was conducted 5 weeks post-AAV injection and thereafter, a 1-week period was given to wash out any effect of the functional testing. On week 6 after the AAV injection, the tibialis anterior muscle was used for high-resolution respirometry and frozen for histology. The gastrocnemius muscle was collected for verification of NOR-1 overexpression and RNA isolation qPCR analysis of putative NOR-1 targets. (B) mRNA expression of NOR-1 in GFP AAV versus NOR-1 AAV-injected gastrocnemius ($n = 8$/group). (C) NOR-1 protein content of GFP AAV and NOR-1 AAV-injected gastrocnemius muscles ($n = 8$/group. (D) Analysis of NOR-1 protein content in livers of mice injected with NOR-1 AAV versus vehicle (PBS) ($n = 3$/group). HPRT was used as a housekeeping gene. Data are presented as Mean ± SEM. Ratio paired *t*-test was used to analyze (B and C) and unpaired *t*-test was used to analyze (D). Statistical significance was set to $p < 0.05$. ***$p < 0.001$, ****$p < 0.0001$. (A) Made with Biorender.com (Created in BioRender. Paez, H. (2024) https://BioRender.com/n43b575).

### 2.9 | NOR-1 Overexpression In Vivo

The tibialis anterior and gastrocnemius muscles from aged (24-month-old) male C57BL6 mice were injected with AAV9 particles ($4\times10^{11}$ and $6\times10^{11}$ particles respectively) to express the NOR-1 transcript linked to an eGFP protein via a T2A linker under control of the CMV promoter (Vector map can be found in Figure 2A). The contralateral limb was injected with AAV9- eGFP particles to express the eGFP transcript driven by the CMV promoter as an intra-animal control. Functional testing was completed 5 weeks after the AAV injection, and tissue harvest and high-resolution respirometry were completed at 6 weeks after AAV injection after a 5-h fast (The timeline can be found in Figure 3A).

To determine if our intramuscular AAV injection led to off-target expression, we measured NOR-1 protein content in the livers of AAV- versus PBS-injected animals. The liver was chosen due to the tropism of our AAV9 serotype towards liver cells.

### 2.10 | Acute Exercise Protocols

Acute treadmill exercise was performed in 5-month-old male and female C57BL6 mice. Briefly, mice were fasted for 1 h before the initiation of exercise. After a 5-min warm-up at 5 m per minute (m/min), treadmill speed remained constant at 12 m/min with a constant grade of 3% for either 15, 30, or 45 min (Experimental design can be found in Figure 1A). One hour after the acute bout of exercise, gene expression of NOR-1 was measured in the gastrocnemius muscle. Control animals were not exercised but did not have access to food for 3 h prior to tissue harvest. Expression of NOR-1 was then quantified in the gastrocnemius muscle utilizing qPCR with Hypoxanthine-guanine phosphoribosyltransferase (HPRT) as the housekeeping gene. To determine how the intensity of exercise modulates NOR-1 expression, 5-month-old male and female C57BL6 mice were anesthetized with isoflurane. Electrically-stimulated plantar flexion was induced by placing subcutaneous electrodes on either side of the tibial nerve and delivering stimulation (200-μs pulse width) at 10, 25, or 50 Hz stimulation frequency (Aurora Scientific, Aurora, Canada). These represented submaximal plantar flexion contractions, as maximal force is generated at 100 Hz [37, 39]. The experimental design for the exercise can be found in Figure 1C. An example of a plantar flexor force record showing a stimulation-dependent increase in submaximal contraction intensity is shown in Figure 1D. Electrically evoked muscle contractions were obtained with the paw of each animal secured to the footplate of the dynamometer with the ankle positioned at 90° flexion to induce an isometric contraction. The isometric exercise protocol consisted of five sets of eight repetitions of isometric contractions with 1 s of rest between repetitions and 2 min of rest between sets to mimic human resistance exercise. Animals were then returned to their cages to rest for 1 h prior to tissue harvest. All animals, including controls, were not given access to food 1 h prior to the exercise protocol or during recovery.

### 2.11 | Muscle Function Testing

Both limbs (NOR-1 and GFP AAV injected) were assessed for measurements of peak torque and fatigability 5 weeks after AAV injection (the timeline for the assessment is shown in Figure 3A). After anesthetization with isoflurane, the hindlimb was immobilized with the ankle positioned at 90° flexion and taped onto a footplate of a dynamometer (Aurora Scientific). Subcutaneous electrodes were placed adjacent to the tibial nerve and delivered stimulation (200μs pulse width) at 100 Hz to generate maximal evoked force. After a 3-min recovery period, muscle fatigue was assessed via a series of 75 contractions at 40 Hz stimulation frequency and 0.1s duration with 200μs pulse width. Between each contraction, there was a 1s delay. We assessed fatigue using approaches that have been modified from a previously described protocol [39]. Briefly, muscle force generated by repeated 40 Hz evoked contractions initially decreases rapidly over the first ~25 contractions in a non-linear fashion ($R^2 \geq 0.98$). Then force declines linearly as a second phase over the contractile record ($R^2 \leq 0.98$) after the initial non-linear decline in force. Finally, in the third phase, the loss of force occurs more rapidly (non-linear) at the end of the contraction protocol. We calculated the rate of fatigue as the slope of the force record (loss of force over time) over the linear portion of the 40 Hz contractile record. The non-linear regions of the force-fatigue curve was not assessed in this study.

Torque data were analyzed offline (Labchart software, ADInstruments) and normalized to the collective weight of the plantar flexor muscles (gastrocnemius, soleus, and plantaris). Data from the fatigue test were normalized to the peak torque produced during the series of contractions. The slope (delta force [df]/delta time [dT]) of the linear portion ($R^2 \geq 0.98$) of the decline in force was used as an estimate of the rate of fatigue.

### 2.12 | Statistics

Results are reported as mean ± SEM. Data between GFP and NOR-1 expressing myotubes were analyzed using an unpaired *t*-test, with the exception of data involving siRNA-mediated PERM1 K.D., which was analyzed via One-Way ANOVA analyses with Tukey's post hoc multiple comparisons test. In vivo, data was analyzed using ratio paired *t*-test to compare NOR-1 AAV-injected muscle to contralateral GFP-injected muscle or One-Way ANOVA to compare NOR-1 responsiveness to exercise. Data comparing NOR-1 content between ages and in the livers of AAV-injected and PBS-injected animals was analyzed via unpaired *t*-test. Data were tested for normality using the Shapiro–Wilk test. When the assumption of normality was violated, data involving more than two groups was analyzed using the non-parametric Kruskal–Wallis test with Dunn's post hoc test or the Brown-Forsythe and Welch ANOVA with Dunnet's post hoc test when the variance between groups was unequal. If normality was violated in comparisons of two groups, the Wilcoxon rank test was used for paired data and the Mann–Whitney test was used for unpaired data. Different letters (A, B, C) denote significant differences between groups. Statistical analyses were performed using GraphPad Prism. Statistical significance was set at $p \leq 0.05$ and effect sizes were calculated using Cohen's d (d). All analyses were performed with the investigator blinded to treatment groups.

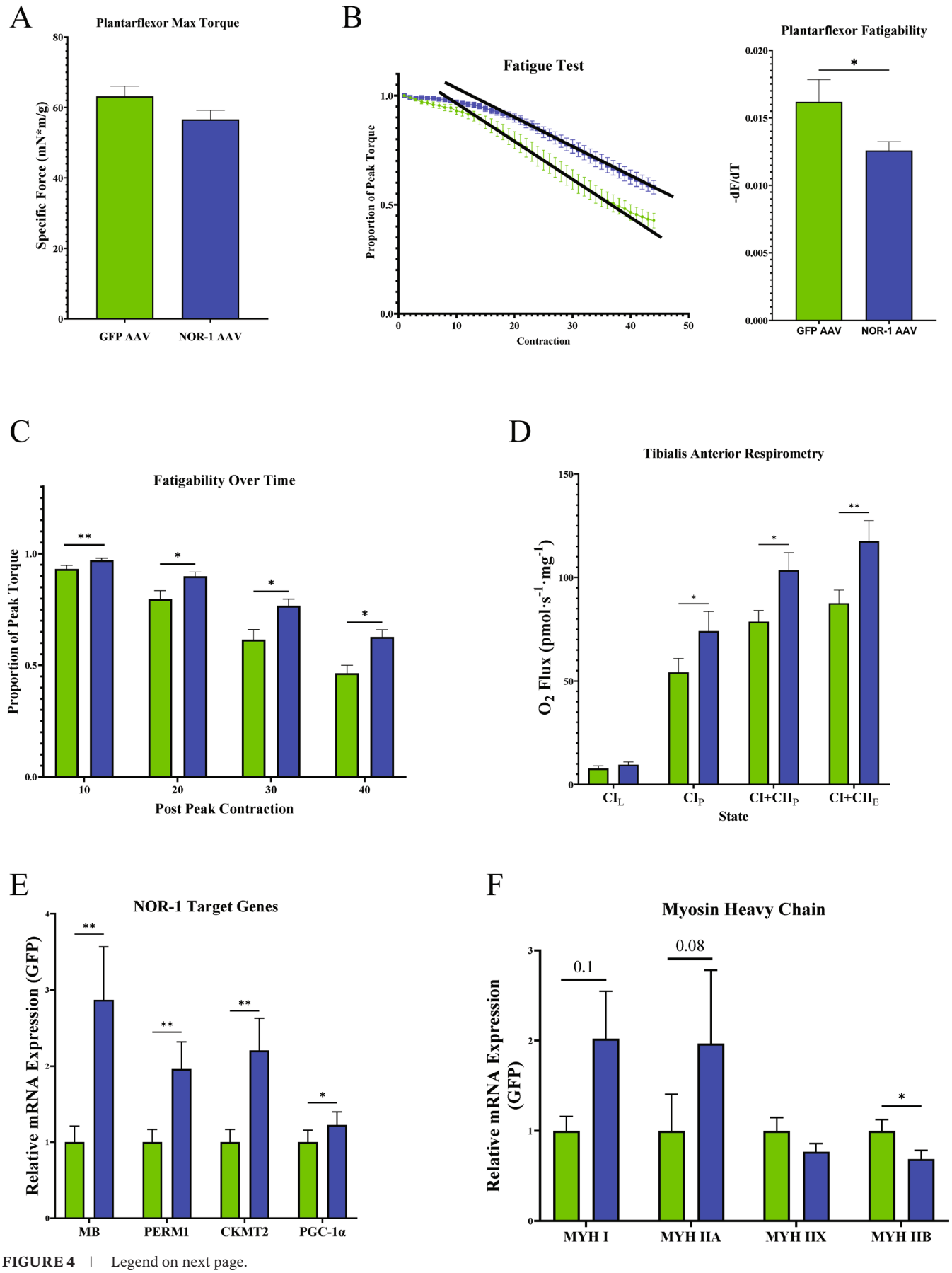


**FIGURE 4** | Legend on next page.

**FIGURE 4** | Impact of NOR-1 overexpression on muscle function and target gene expression in vivo. (A) Specific torque production measured between NOR-1 and GFP AAV-injected limbs ($n = 10$/group). (B) Fatigue test showing the drop in force production after reaching peak torque between GFP and NOR-1 AAV-injected limbs ($n = 10$/group) and the fatigability represented as the negative change in force (−dF) over the change in time (dT) during the linear portion of the drop in force during the fatigue test ($n = 10$/group). (C) Proportion of peak force sustained at various points after reaching the peak contraction during the fatigue test ($n = 10$/group). (D) High-resolution respirometry of tibialis anterior permeabilized fibers ($n = 8$/group). (E) Gene expression of NOR-1 target genes in AAV-injected gastrocnemius ($n = 8$/group). (F) Myosin heavy chain isoform gene expression in gastrocnemius muscle ($n = 8$/group). HPRT was used as a housekeeping gene. Data is presented as Mean ± SEM. Ratio paired *t*-test and Wilcoxon Rank paired test were used to analyze data. Statistical significance was set to $p < 0.05$. $^{*}p < 0.05$, $^{**}p < 0.01$.

## 3 | Results

### 3.1 | Expression of NOR-1 Is Responsive to Exercise Dose but Impaired in Aged Skeletal Muscle

NOR-1 responsiveness to acute exercise and muscle contraction is well established [17, 23]. However, whether NOR-1 expression is responsive to the duration or intensity of exercise is unknown. Furthermore, exercise is known to be a potent intervention to improve muscle function in aged persons [8], in part by reversing age-associated changes in muscle [10, 11, 40]. It is unknown if aging is associated with deficient NOR-1 expression in skeletal muscle. To test whether the duration of exercise influences the degree of NOR-1 expression in skeletal muscle, young (5 months of age) male and female mice performed a bout of moderate aerobic exercise via treadmill running for either 15, 30, or 45 min (Figure 1A). One hour after the acute bout of exercise, gene expression of NOR-1 was measured in the gastrocnemius muscle. In as little as 15 min of running, NOR-1 expression was ~2.5 times greater than controls, although this did not reach statistical significance ($p = 0.3191$; $d = 2.06$). However, 30 min of treadmill exercise resulted in a ~3-fold enhancement ($p = 0.049$; $d = 3.46$), and 45 min of exercise led to a ~7-fold increase ($p = 0.0013$; $d = 1.79$) in NOR-1 expression (Figure 1B). These data would indicate that at a moderate intensity, aerobic exercise elevates NOR-1 expression in a duration-dependent fashion. To evaluate whether NOR-1 expression is similarly responsive to the intensity of exercise, animals underwent an acute bout of electrically evoked isometric exercise (Figure 1C). Interestingly, we observed that, in addition to being responsive to the duration of exercise, NOR-1 expression in the gastrocnemius exhibited an intensity-dependent increase in response to submaximal isometric muscle contractions (Figure 1E). Expression of NOR-1 was elevated by ~2.6-fold following contractions at 10 Hz, but this did not reach statistical significance ($p = 0.184$; $d = 3.35$). In contrast, stimulation at 25 Hz and 50 Hz led to a ~4.7-fold ($p = 0.0007$; $d = 4.03$) and ~6-fold ($p < 0.0001$; $d = 3.59$) enhancement in NOR-1 expression, respectively. In contrast to the elevation in NOR-1 expression by exercise, aged (male and female, 27–31 months of age) mice had 45% ($d = -1.47$) lower NOR-1 gene expression relative to young adult mice (male and female mice aged 9 months) in the plantaris muscle (Figure 1F).

### 3.2 | Inhibition of PERM1 Ablates the Enhancement of Myoglobin but Not CKMT2 Expression by NOR-1

Deficiencies in NOR-1 expression are associated with impaired expression of several genes important for oxidative metabolism [27]. We next asked if overexpression of NOR-1 in vitro would elevate genes associated with metabolism; thus, we infected C2C12 myotubes (day 3 of differentiation) with AAV9 particles to express NOR-1 linked to an eGFP protein via a T2A linker under the control of the CMV promoter (Figure 2A). Cells infected with AAV9 particles to express eGFP under the control of the CMV promoter were used as controls. Visualization of cells showed robust GFP fluorescence in myotubes 7 days post-transduction (Figure 2B) and approximately 94-fold enhancement of NOR-1 gene expression (Figure 2C). We then measured the expression of several genes associated with oxidative metabolism that we had previously identified as being downregulated after NOR-1 K.D. [27]. We found several genes that facilitate mitochondrial function (MFN2, ATP5A1, COQ3, TFAM, and ANT1) were moderately upregulated. We also observed an upregulation of PGC-1α, which is consistent with published findings [25, 27]. Notably, we observed large changes in the expression of three genes associated with oxidative function in skeletal muscle including CKMT2 (+205%, $p = 0.0011$; $d = 2.61$), myoglobin (+257%, $p < 0.0001$; $d = 4.57$), and PERM1 (+345%, $p < 0.0001$; $d = 4.81$) after NOR-1 overexpression (Figure 2D).

PERM1 is known to regulate mitochondrial localization [29], function [30], and exercise adaptations [31] and was among the most upregulated genes in animals that overexpress hyperactive NOR-1 [28]. Therefore, we asked if the NOR-1-induced changes to CKMT2 and myoglobin expression require elevated PERM1 expression. To answer this question, we utilized AAV-mediated overexpression of NOR-1 in combination with siRNA K.D. of PERM1 (Experimental design shown in Figure 2E). In myotubes which were transduced with GFP AAV, PERM1 siRNA treatment resulted in approximately an 85% reduction in PERM1 gene expression ($p < 0.0001$; $d = -4.51$) (Figure 2F). In control siRNA-transfected cells, NOR-1 AAV led to a 310% increase in PERM1 expression when compared to GFP AAV transduced cells ($p < 0.001$; $d = 10.15$). However, NOR-1 AAV-treated cells that were transfected with PERM1-targeting siRNA exhibited a 79% reduction in PERM1 gene expression ($p < 0.0001$; $d = -11.12$). Importantly, relative to GFP AAV transduced cells which were transfected with the control siRNA, NOR-1 AAV transduced cells which were transfected with PERM1 siRNA expressed a similar degree of PERM1 ($p = 0.8589$; $d = -0.46$). This would indicate that our design and degree of K.D. ensured that PERM1 expression in our NOR-1 AAV transduced cells after PERM1 siRNA transfection was comparable to the expression in our GFP-transduced cells after control siRNA transfection, and any changes detected would not be due to excessively low PERM1 expression. When measuring the expression of CKMT2, we found that PERM1 K.D. did not affect CKMT2

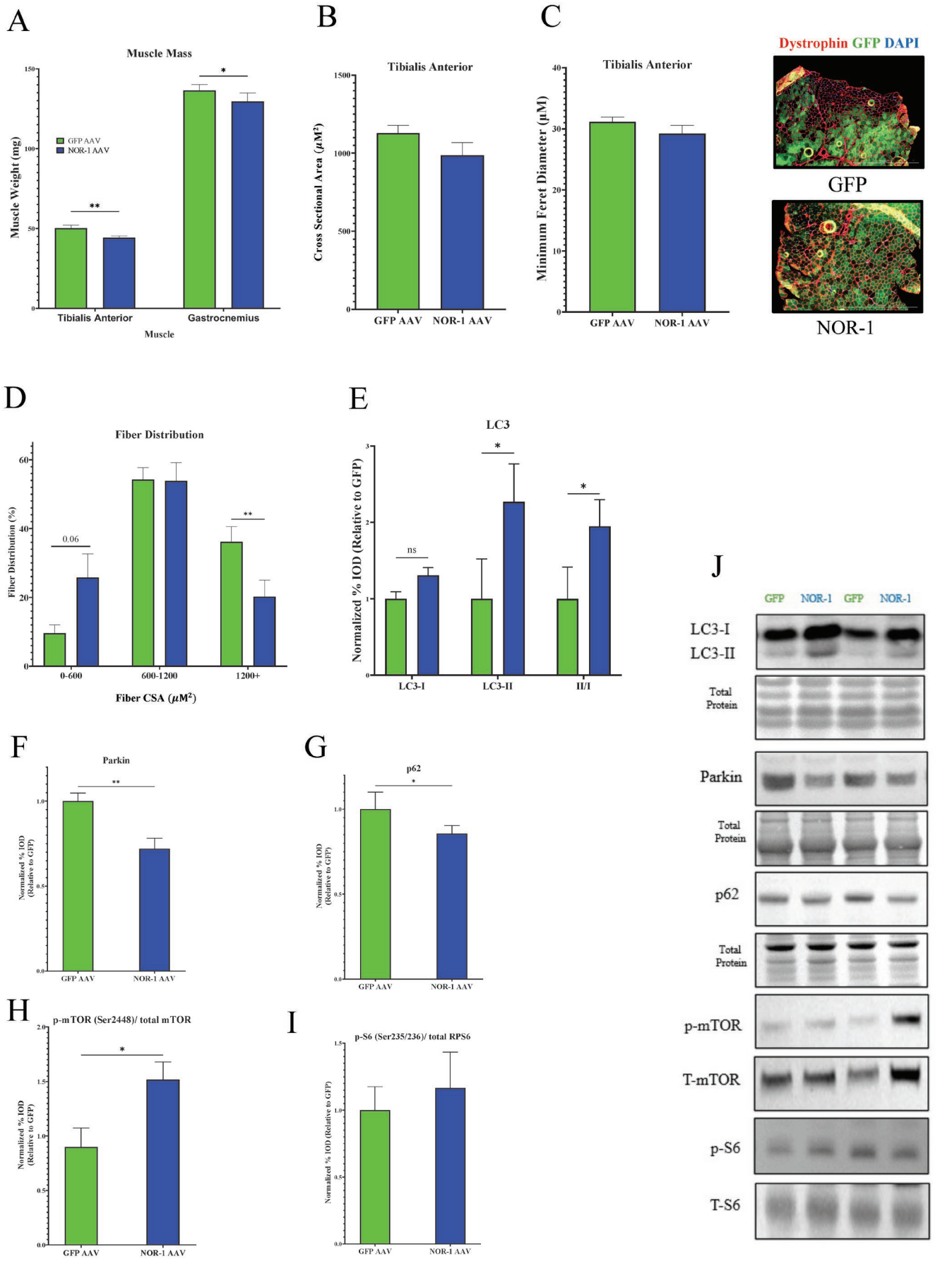


**FIGURE 5** | Legend on next page.

**FIGURE 5** | Impact of NOR-1 overexpression on muscle size and signaling in aged skeletal muscle. (A) Muscle wet weight of tibialis anterior and gastrocnemius muscles 6 weeks after AAV injection ($n = 11$/group). (B) Average cross-sectional area (CSA) and (C) minimum feret diameter of GFP+ fibers in the tibialis anterior ($n = 8$/group) and representative image of GFP+ fibers (scale bar is 1000 μM). (D) Fiber distribution of fibers that were categorized into small (0–600 $\mu m^2$), medium (600–1200 $\mu m^2$), or large (1200+ $\mu m^2$) fiber CSA in the tibialis anterior ($n = 8$/group). Western blot analysis of gastrocnemius muscle for (E) LC3-I/II, (F) Parkin, (G) p62, and the phosphorylation status of (H) mTORC1 at Ser2448 and its downstream target (I) S6 at Ser235/236. (J) Representative blots. Data is presented as Mean ± SEM. Ratio paired *t*-test and Wilcoxon Rank paired test were used to analyze data. Statistical significance was set to $p < 0.05$. $^*p < 0.05$, $^{**}p < 0.01$.

expression in either GFP-transduced or NOR-1 transduced cells (Figure 2G), although we did detect significantly greater CKMT2 expression after NOR-1 AAV transduction regardless of siRNA transfection; indicating that NOR-1 elevates expression of CKMT2 regardless of the degree of PERM1 expression. We observed a greater than three-fold increase in myoglobin expression with NOR-1 AAV transduction as compared to control AAV transduced cells ($p = 0.0006$; $d = -4.42$) (Figure 2H). K.D. of PERM1 did not decrease myoglobin gene expression in GFP-transduced cells ($p = 0.9889$; $d = 0.34$). However, K.D. of PERM1 completely ablated the enhancement of myoglobin expression that occurred with NOR-1 AAV transduction. PERM1 K.D. reduced myoglobin expression in NOR-1 AAV transduced cells by 80% ($p < 0.0001$; $d = 11.67$). We found that after PERM1 K.D., NOR-1 AAV-treated cells expressed a similar degree of myoglobin as compared to GFP-transduced cells that were transfected with our control siRNA ($p = 0.4924$; $d = -1.00$). Taken together, these data indicate that the NOR-1-mediated increase of myoglobin, but not CKMT2, occurs in a PERM1-dependent fashion.

### 3.3 | Overexpression of NOR-1 In Vivo

We then asked if NOR-1 AAV treatment in vivo would enhance skeletal muscle PERM1, CKMT2, PGC-1α, and myoglobin expression and whether this would be associated with changes to muscle function in aged animals. To answer this question, we injected the tibialis anterior and gastrocnemius of aged (24-month-old) male and female mice with NOR-1 AAV and the contralateral tibialis anterior and gastrocnemius with GFP AAV as an intranimal control. We then tested the peak torque and fatigability of plantar flexors 5 weeks after AAV injections. Tissue harvest and high-resolution respirometry were conducted 1 week after functional testing (Experimental design shown in Figure 3A). Relative to GFP-injected gastrocnemius muscles, NOR-1 AAV significantly enhanced NOR-1 gene expression (72-fold, $p < 0.0001$; $d = 2.36$) (Figure 3B) and protein abundance (2.2-fold, $p = 0.0006$; $d = 3.63$) (Figure 3C). We did not observe greater NOR-1 protein abundance in the livers of AAV-injected versus PBS-injected animals ($p = 0.8497$; $d = 0.17$) (Figure 3D).

### 3.4 | NOR-1 Overexpression Enhances Skeletal Muscle Mitochondrial Function but Not Peak Force

After successfully overexpressing NOR-1 in the skeletal muscle of aged mice, we asked whether this would be associated with enhanced muscle function. We did not find a significant difference in peak plantar flexor torque (Figure 4A). However, an analysis of the rate of force drop-off during the linear decline of our fatigue test (Figure 4B) revealed that NOR-1 AAV-injected limbs fatigued at a lower rate than the GFP AAV-injected limbs ($p = 0.0371$; $d = -0.90$). Furthermore, an analysis of the ability to maintain torque after 10, 20, 30, and 40 contractions after reaching peak torque revealed that NOR-1 AAV-injected limbs maintained a higher relative torque than GFP-injected limbs (Figure 4C), indicating an elevated capacity to sustain contraction intensity (i.e., increased work and reduced fatigue) during repeated bouts of contraction. To determine whether NOR-1 overexpression also resulted in greater mitochondrial function, we performed high-resolution respirometry of the tibialis anterior muscle. We did not observe any changes to complex I-supported leak ($p = 0.4213$; $d = 0.07$); however, we did observe that NOR-1 AAV-injected tibialis anterior muscle had greater complex I ($p = 0.0231$; $d = 0.85$) and complex I + II supported OXPHOS respiration ($p = 0.0215$; $d = 1.22$) and maximal CI + CII electron transport system capacity ($p = 0.0075$; $d = 1.25$) (Figure 4D). In agreement with our in vitro experiments, we found elevated gene expression for myoglobin ($p = 0.0011$; $d = 1.28$), PERM1 ($p = 0.0039$; $d = 1.23$), CKMT2 ($p = 0.0021$; $d = 1.32$), and PGC-1α ($p = 0.0492$; $d = 0.48$) in the gastrocnemius muscle of NOR-1 versus GFP AAV-injected muscle (Figure 4E). Interestingly, we found that NOR-1 AAV led to a significant reduction in myosin heavy chain IIB expression ($p = 0.0404$; $d = -1.00$) and a strong trend for elevated myosin heavy chain type I ($p = 0.1094$; $d = 0.93$) and type IIA ($p = 0.0844$; $d = 0.53$) expression (Figure 4F). These data indicate that NOR-1 overexpression may shift myosin heavy chain isoform gene expression away from glycolytic fiber types towards smaller and slower, more oxidative fiber types.

### 3.5 | Impact of NOR-1 Overexpression on Muscle Size and Autophagy Signaling

Exercise is an effective means to combat sarcopenia [41]. Thus, we were also interested in determining how NOR-1 overexpression altered muscle mass. Interestingly, we found a small but statistically significant reduction in muscle wet weight in the gastrocnemius (−5%, $p = 0.0159$; $d = -0.45$) and the tibialis anterior (−12%, $p = 0.0033$; $d = -1.23$) (Figure 5A). When analyzing the cross-sectional area (CSA) (Figure 5B) and minimum feret diameter (Figure 5C) of GFP+ fibers, we did not find a significant reduction in fiber size, although there was a strong trend for lower average CSA in NOR-1 AAV-treated fibers ($p = 0.0698$; $d = -0.74$). A closer analysis of fiber size distributions of GFP+ fibers revealed a strong trend towards a greater proportion of smaller (0–600 $\mu m^2$) fibers in NOR-1 AAV-injected tibialis anterior fibers ($p = 0.0609$; $d = 1.11$) alongside no changes in medium (600–1200 $\mu m^2$) sized fibers ($p = 0.7986$; $d = 0.03$) and

a significantly lower proportion of large (1200+ $\mu m^2$) fibers ($p = 0.0085$; $d = -1.22$) (Figure 5D). We have previously shown that NOR-1 K.D. impairs mTORC1 signaling [27] and previous evidence implicates NOR-1 in the regulation of autophagy [24]. Thus, we asked if these changes in myofiber size were associated with alterations in mTORC1 or autophagy signaling. We observed that NOR-1 overexpression resulted in significantly elevated LC3-II and LC3-II/I ratio but not LC3-I (Figure 5E). Furthermore, we detected significantly reduced Parkin protein abundance (Figure 5F) and a small but statistically significant reduction in p62 protein content (Figure 5G). Paradoxically, we also detected elevated phosphorylation of mTOR (Figure 5H); however, we did not detect any changes in the phosphorylation status of the downstream mTORC1 target ribosomal protein S6 (Figure 5I). Taken together, these data suggest that chronic overexpression of NOR-1 in aged skeletal muscle results in a slight but statistically significant decrease in muscle mass that coincides with a shift towards an oxidative type I fiber phenotype, elevated autophagy signaling, and mTOR phosphorylation.

## 4 | Discussion

Skeletal muscle aging is associated with deficits in mitochondrial function [42], impaired muscle function [43–45], and reduced muscle mass [46]. Currently, exercise is among the most effective interventions to improve muscle function and mass in aged persons [8, 41]. However, vigorous exercise may not be a feasible treatment in some elderly people due to mobility impairments, comorbidities, or low attrition. Thus, the study of exercise-mediated benefits is important to broaden our understanding of the mechanistic underpinnings of exercise and identify health-promoting druggable targets. Although the responsiveness of NOR-1 to acute exercise has been appreciated for over two decades [47], we extend these findings and dissect how exercise of varying modalities, durations, and intensities alters the expression of NOR-1. Furthermore, we observed that aged skeletal muscle exhibits impaired NOR-1 expression. Our data agree with previous findings that NOR-1 K.D. reduces PGC-1α expression [25] and that mice that overexpress NOR-1 have elevated myoglobin expression [35]. Furthermore, we uncovered a signaling axis by which NOR-1 upregulates myoglobin expression in a PERM1-dependent manner. Previous reports on the effects of NOR-1 overexpression on muscle endurance have utilized treadmill running performance [35], which relies heavily on both skeletal muscle and cardiovascular performance. Using direct muscle stimulation, we show that NOR-1 overexpression directly improves muscle fatigability. Furthermore, this was concomitant with improved mitochondrial respiration. We did not observe a statistically significant change in peak torque with NOR-1 overexpression. One unexpected finding was that overexpression of NOR-1 resulted in reduced muscle mass and a lower proportion of large fibers. This might have been the result of a phenotype shift towards smaller, more oxidative type I fibers. It is known that phosphorylation of NOR-1 can induce nuclear export and mitochondrial localization [48, 49], although the significance of post-translational modifications to NOR-1 in skeletal muscle is unknown. It is possible that our use of the CMV promoter, although advantageous for achieving high NOR-1 expression, may produce NOR-1 overexpression in motor neurons or resident mononuclear cells in skeletal muscle (immune cells, satellite cells, fibroblasts, etc.) that may negatively impact muscle mass. Interestingly, although we did not aim to define the mechanism by which NOR-1 alters muscle mass, we did find that there were signs of elevated autophagy in NOR-1 AAV transduced muscle. We observed an elevation in LC3-II and LC3-II/I ratio alongside a moderate decline in Parkin and p62 protein abundance. It is possible that a subset of fibers that were infected within the muscle may have exhibited an elevation in autophagy and subsequent atrophy, as animals that overexpress NOR-1 also show signs of heightened autophagy [24] including elevated skeletal muscle LC3-II and reduced p62 content.

We recognize that our study has several limitations. First, our use of a CMV promoter, while important to achieve a high degree of NOR-1 expression, meant that other cells within the injected muscle could have likely also overexpressed NOR-1. Therefore, we cannot rule out that non-muscle cells that overexpressed NOR-1 contributed to improvements or deficits in muscle mass or function. However, it is important to keep in mind that pharmacological strategies to enhance NOR-1 expression or activity are also likely to impact non-muscle tissues. Another limitation is that we used only isometric contractions in this study. It is possible that isokinetic or concentric muscle function may have enhanced or altered responses to NOR-1 as compared to isometric contractions. A final limitation was that while we did not conduct fiber-type specific analyses, we were unable to determine if NOR-1 was translated more efficiently in a fiber-type specific fashion. Nevertheless, our findings suggest that NOR-1 overexpression can improve muscle fatigability during isometric exercise and maximal mitochondrial respiration. Although improved muscle endurance and skeletal muscle mitochondrial function can be beneficial to aged people, it is also important to note that aging and sarcopenia are frequently associated with fast muscle fiber atrophy, reductions in peak force, and reduced muscle mass. While some of the effects of NOR-1 overexpression could potentially exacerbate some of the detrimental aspects of aging on skeletal muscle by inducing a phenotype shift towards a smaller oxidative phenotype and contributing to lower muscle weight, an increased distribution of type I fibers would be expected to be more resistant to further sarcopenia. Furthermore, it is known that NOR-1 is a regulator of neuronal survival [50] and that dysfunction of the motor neuron is a main contributor to aging-associated muscle dysfunction [5]. It is interesting to note that specific force was not altered by NOR-1 overexpression despite reductions in muscle mass. Understanding whether NOR-1 alters the neuromuscular junction will provide insight into potential mechanisms by which exercise and NOR-1 impact muscle function. Additional work is needed to address these questions including studies using transgenic mice and mutant forms of NOR-1 (i.e., phospho-incompetent NOR-1) that will be necessary to further dissect the function and therapeutic potential of NOR-1 for skeletal muscle-associated pathologies.

### Author Contributions

Experiments were designed by H.G.P. and S.E.A. Experiments were conducted by H.G.P. Statistical analysis and figure preparation were completed by H.G.P. and S.E.A. Manuscript preparation was conducted by H.G.P., S.E.A., C.R.P., J.S.M., and P.J.F. Manuscript review and editing were conducted by H.G.P., C.R.P., J.S.M., P.J.F., and S.E.A.

**Acknowledgments**

A.A.V. production was conducted by VectorBuilder and the AAV vector map was created using VectorBuilder software. The antibody MandyS8(8H11) was developed by G.E. Morris. This antibody was obtained from the Developmental Studies Hybridoma Bank developed under the auspices of the NICHD and maintained by the University of Iowa, Department of Biology, Iowa City, IA 52242, USA. Experimental design figures were created with Biorender.com.

**Conflicts of Interest**

The authors declare no conflicts of interest.

**Data Availability Statement**

The data that support the findings of this study are available from the corresponding author upon reasonable request.

**References**

1. H. Arem, S. C. Moore, A. Patel, et al., "Leisure Time Physical Activity and Mortality: A Detailed Pooled Analysis of the Dose-Response Relationship," *JAMA Internal Medicine* 175 (2015): 959–967.

2. C. A. Slentz, J. A. Houmard, and W. E. Kraus, "Modest Exercise Prevents the Progressive Disease Associated With Physical Inactivity," *Exercise and Sport Sciences Reviews* 35 (2007): 18–23.

3. M. Narici, G. Vito, M. Franchi, et al., "Impact of Sedentarism due to the COVID-19 Home Confinement on Neuromuscular, Cardiovascular and Metabolic Health: Physiological and Pathophysiological Implications and Recommendations for Physical and Nutritional Countermeasures," *European Journal of Sport Science* 21 (2021): 614–635.

4. R. Nilwik, T. Snijders, M. Leenders, et al., "The Decline in Skeletal Muscle Mass With Aging Is Mainly Attributed to a Reduction in Type II Muscle Fiber Size," *Experimental Gerontology* 48 (2013): 492–498.

5. S. E. Alway, J. S. Mohamed, and M. J. Myers, "Mitochondria Initiate and Regulate Sarcopenia," *Exercise and Sport Sciences Reviews* 45 (2017): 58–69, https://doi.org:10.1249/JES.0000000000000101.

6. A. Picca, M. Triolo, S. E. Wohlgemuth, et al., "Relationship Between Mitochondrial Quality Control Markers, Lower Extremity Tissue Composition, and Physical Performance in Physically Inactive Older Adults," *Cells* 12 (2023): 183, https://doi.org:10.3390/cells12010183.

7. A. M. Joseph, P. J. Adhihetty, T. W. Buford, et al., "The Impact of Aging on Mitochondrial Function and Biogenesis Pathways in Skeletal Muscle of Sedentary High-and Low-Functioning Elderly Individuals," *Aging Cell* 11 (2012): 801–809.

8. S. E. Alway, J. L. McCrory, K. Kearcher, et al., "Resveratrol Enhances Exercise-Induced Cellular and Functional Adaptations of Skeletal Muscle in Older Men and Women," *Journals of Gerontology. Series A, Biological Sciences and Medical Sciences* 72 (2017): 1595–1606.

9. A. R. Konopka, M. K. Suer, C. A. Wolff, and M. P. Harber, "Markers of Human Skeletal Muscle Mitochondrial Biogenesis and Quality Control: Effects of Age and Aerobic Exercise Training," *Journals of Gerontology. Series A, Biological Sciences and Medical Sciences* 69 (2014): 371–378.

10. C. Kang, E. Chung, G. Diffee, and L. L. Ji, "Exercise Training Attenuates Aging-Associated Mitochondrial Dysfunction in Rat Skeletal Muscle: Role of PGC-1α," *Experimental Gerontology* 48 (2013): 1343–1350.

11. E. Koltai, N. Hart, A. W. Taylor, et al., "Age-Associated Declines in Mitochondrial Biogenesis and Protein Quality Control Factors Are Minimized by Exercise Training," *American Journal of Physiology-Regulatory, Integrative and Comparative Physiology* 303 (2012): R127–R134.

12. A. Vainshtein and D. A. Hood, "The Regulation of Autophagy During Exercise in Skeletal Muscle," *Journal of Applied Physiology* 120 (2016): 664–673.

13. C. C. W. Chen, A. T. Erlich, and D. A. Hood, "Role of Parkin and Endurance Training on Mitochondrial Turnover in Skeletal Muscle," *Skeletal Muscle* 8 (2018): 1–14.

14. H. G. Paez, C. R. Pitzer, and S. E. Alway, "Age-Related Dysfunction in Proteostasis and Cellular Quality Control in the Development of Sarcopenia," *Cells* 12 (2023): 249.

15. Z. Zeng, J. Liang, L. Wu, H. Zhang, J. Lv, and N. Chen, "Exercise-Induced Autophagy Suppresses Sarcopenia Through Akt/mTOR and Akt/FoxO3a Signal Pathways and AMPK-Mediated Mitochondrial Quality Control," *Frontiers in Physiology* 11 (2020): 583478.

16. C. S. Fry, M. J. Drummond, E. L. Glynn, et al., "Aging Impairs Contraction-Induced Human Skeletal Muscle mTORC1 Signaling and Protein Synthesis," *Skeletal Muscle* 1 (2011): 1–11.

17. N. J. Pillon, B. M. Gabriel, L. Dollet, et al., "Transcriptomic Profiling of Skeletal Muscle Adaptations to Exercise and Inactivity," *Nature Communications* 11 (2020): 1–15.

18. I. Ohsawa and F. Kawano, "Chronic Exercise Training Activates Histone Turnover in Mouse Skeletal Muscle Fibers," *FASEB Journal* 35 (2021): e21453.

19. D. Mahoney, G. Parise, S. Melov, A. Safdar, and M. Tarnopolsky, "Analysis of Global mRNA Expression in Human Skeletal Muscle During Recovery From Endurance Exercise," *FASEB Journal* 19 (2005): 1498–1500.

20. M. F. Maasar, D. C. Turner, P. P. Gorski, et al., "The Comparative Methylome and Transcriptome After Change of Direction Compared to Straight Line Running Exercise in Human Skeletal Muscle," *Frontiers in Physiology* 12 (2021): e619447.

21. M. Catoire, M. Mensink, M. V. Boekschoten, et al., "Pronounced Effects of Acute Endurance Exercise on Gene Expression in Resting and Exercising Human Skeletal Muscle," *PLoS One* 7 (2012): e51066.

22. H. C. Rundqvist, A. Montelius, T. Osterlund, B. Norman, M. Esbjornsson, and E. Jansson, "Acute Sprint Exercise Transcriptome in Human Skeletal Muscle," *PLoS One* 14 (2019): e0223024.

23. P. Pattamaprapanont, C. Garde, O. Fabre, and R. Barrès, "Muscle Contraction Induces Acute Hydroxymethylation of the Exercise-Responsive Gene Nr4a3," *Frontiers in Endocrinology* 7 (2016): 165.

24. J. M. Goode, M. A. Pearen, Z. K. Tuong, et al., "The Nuclear Receptor, Nor-1, Induces the Physiological Responses Associated With Exercise," *Molecular Endocrinology* 30 (2016): 660–676.

25. M. A. Pearen, S. A. Myers, S. Raichur, J. G. Ryall, G. S. Lynch, and G. E. Muscat, "The Orphan Nuclear Receptor, NOR-1, a Target of β-Adrenergic Signaling, Regulates Gene Expression That Controls Oxidative Metabolism in Skeletal Muscle," *Endocrinology* 149 (2008): 2853–2865.

26. M. A. Pearen, J. G. Ryall, M. A. Maxwell, N. Ohkura, G. S. Lynch, and G. E. Muscat, "The Orphan Nuclear Receptor, NOR-1, Is a Target of β-Adrenergic Signaling in Skeletal Muscle," *Endocrinology* 147 (2006): 5217–5227.

27. H. G. Paez, P. J. Ferrandi, C. R. Pitzer, J. S. Mohamed, and S. E. Alway, "Loss of NOR-1 Represses Muscle Metabolism Through mTORC1-Mediated Signaling and Mitochondrial Gene Expression in C2C12 Myotubes," *FASEB Journal* 37 (2023): e23050.

28. M. A. Pearen, J. M. Goode, R. L. Fitzsimmons, et al., "Transgenic Muscle-Specific Nor-1 Expression Regulates Multiple Pathways That Effect Adiposity, Metabolism, and Endurance," *Molecular Endocrinology* 27 (2013): 1897–1917.

29. T. Bock, C. Türk, S. Aravamudhan, et al., "PERM1 Interacts With the MICOS-MIB Complex to Connect the Mitochondria and Sarcolemma via Ankyrin B," *Nature Communications* 12 (2021): 1–15.

30. Y. Cho, B. C. Hazen, P. G. Gandra, et al., "Perm1 Enhances Mitochondrial Biogenesis, Oxidative Capacity, and Fatigue Resistance in Adult Skeletal Muscle," *FASEB Journal* 30 (2016): 674–687.

31. Y. Cho, S. Tachibana, B. C. Hazen, et al., "Perm1 Regulates CaMKII Activation and Shapes Skeletal Muscle Responses to Endurance Exercise Training," *Molecular Metabolism* 23 (2019): 88–97.

32. K. K. Adepu, A. Anishkin, S. H. Adams, and S. V. Chintapalli, "A Versatile Delivery Vehicle for Cellular Oxygen and Fuels, or Metabolic Sensor? -A Review and Perspective on the Functions of Myoglobin," *Physiological Reviews* 104 (2024): 1611–1642.

33. L. Kay, K. Nicolay, B. Wieringa, V. Saks, and T. Wallimann, "Direct Evidence for the Control of Mitochondrial Respiration by Mitochondrial Creatine Kinase in Oxidative Muscle Cells In Situ," *Journal of Biological Chemistry* 275 (2000): 6937–6944.

34. N. Park, J. Marquez, M. V. F. Garcia, et al., "Phosphorylation in Novel Mitochondrial Creatine Kinase Tyrosine Residues Render Cardioprotection Against Hypoxia/Reoxygenation Injury," *Journal of Lipid and Atherosclerosis* 10 (2021): 223.

35. M. A. Pearen, N. A. Eriksson, R. L. Fitzsimmons, et al., "The Nuclear Receptor, Nor-1, Markedly Increases Type II Oxidative Muscle Fibers and Resistance to Fatigue," *Molecular Endocrinology* 26 (2012): 372–384.

36. J. L. Halle, G. S. Pena, H. G. Paez, et al., "Tissue-Specific Dysregulation of Mitochondrial Respiratory Capacity and Coupling Control in Colon-26 Tumor-Induced Cachexia," *American Journal of Physiology. Regulatory, Integrative and Comparative Physiology* 317 (2019): R68–R82, https://doi.org:10.1152/ajpregu.00028.2019.

37. S. E. Alway, H. G. Paez, C. R. Pitzer, et al., "Mitochondria Transplant Therapy Improves Regeneration and Restoration of Injured Skeletal Muscle," *Journal of Cachexia, Sarcopenia and Muscle* 14 (2023): 493–507, https://doi.org:10.1002/jcsm.13153.

38. Y. Wen, K. A. Murach, I. J. Vechetti, Jr., et al., "MyoVision: Software for Automated High-Content Analysis of Skeletal Muscle Immunohistochemistry," *Journal of Applied Physiology* 124 (2018): 40–51.

39. M. J. Myers, D. L. Shepherd, A. J. Durr, et al., "The Role of SIRT1 in Skeletal Muscle Function and Repair of Older Mice," *Journal of Cachexia, Sarcopenia and Muscle* 10 (2019): 929–949, https://doi.org:10.1002/jcsm.12437.

40. R. M. de Guia, M. Agerholm, T. S. Nielsen, et al., "Aerobic and Resistance Exercise Training Reverses Age-Dependent Decline in NAD+ Salvage Capacity in Human Skeletal Muscle," *Physiological Reports* 7 (2019): e14139.

41. Y. Shen, Q. Shi, K. Nong, et al., "Exercise for Sarcopenia in Older People: A Systematic Review and Network Meta-Analysis," *Journal of Cachexia, Sarcopenia and Muscle* 14 (2023): 1199–1211.

42. S. C. Lewsey, K. Weiss, M. Schär, et al., "Exercise Intolerance and Rapid Skeletal Muscle Energetic Decline in Human Age-Associated Frailty," *JCI Insight* 5 (2020): e141246.

43. S. Baudry, M. Klass, B. Pasquet, and J. Duchateau, "Age-Related Fatigability of the Ankle Dorsiflexor Muscles During Concentric and Eccentric Contractions," *European Journal of Applied Physiology* 100 (2007): 515–525.

44. C. J. McNeil and C. L. Rice, "Fatigability Is Increased With Age During Velocity-Dependent Contractions of the Dorsiflexors," *Journals of Gerontology Series A: Biological Sciences and Medical Sciences* 62 (2007): 624–629.

45. B. J. Thompson, E. D. Ryan, E. J. Sobolewski, E. C. Conchola, and J. T. Cramer, "Age Related Differences in Maximal and Rapid Torque Characteristics of the Leg Extensors and Flexors in Young, Middle-Aged and Old Men," *Experimental Gerontology* 48 (2013): 277–282.

46. J. R. Jackson, M. J. Ryan, and S. E. Alway, "Long-Term Supplementation With Resveratrol Alleviates Oxidative Stress but Does Not Attenuate Sarcopenia in Aged Mice," *Journals of Gerontology. Series A, Biological Sciences and Medical Sciences* 66 (2011): 751–764.

47. A. C. Zambon, E. McDearmon, N. Salomonis, et al., "Time-and Exercise-Dependent Gene Regulation in Human Skeletal Muscle," *Genome Biology* 4 (2003): 1–12.

48. J. Thompson and A. Winoto, "During Negative Selection, Nur77 Family Proteins Translocate to Mitochondria Where They Associate With Bcl-2 and Expose Its Proapoptotic BH3 Domain," *Journal of Experimental Medicine* 205 (2008): 1029–1036.

49. J. Thompson, M. L. Burger, H. Whang, and A. Winoto, "Protein Kinase C Regulates Mitochondrial Targeting of Nur77 and Its Family Member Nor-1 in Thymocytes Undergoing Apoptosis," *European Journal of Immunology* 40 (2010): 2041–2049.

50. J. Gagnon, V. Caron, L. Gyenizse, and A. Tremblay, "Atypic SUMOylation of Nor1/NR4A3 Regulates Neural Cell Viability and Redox Sensitivity," *FASEB Journal* 35 (2021): e21827.